Exp Astron (2012) 33:685–721
DOI 10.1007/s10686-011-9253-2

ORIGINAL ARTICLE

Trojans' Odyssey: Unveiling the early history of the Solar System

Philippe Lamy · Pierre Vernazza · Joel Poncy · Vincent Martinot · Emmanuel Hinglais · Elisabet Canalias · Jim Bell · Dale Cruikshank · Olivier Groussin · Joern Helbert · Francesco Marzari · Alessandro Morbidelli · Pascal Rosenblatt · Holger Sierks

Received: 31 March 2011 / Accepted: 4 August 2011 / Published online: 3 September 2011

Abstract In our present understanding of the Solar System, small bodies (asteroids, Jupiter Trojans, comets and TNOs) are the most direct remnants of the original building blocks that formed the planets. Jupiter Trojan and Hilda

P. Lamy (✉) · P. Vernazza · O. Groussin
Laboratoire d'Astrophysique de Marseille, 38 rue Frédéric Joliot-Curie,
13388 Marseille, France
e-mail: philippe.lamy@oamp.fr

J. Poncy · V. Martinot
Thales Alenia Space, Cannes, France

E. Hinglais · E. Canalias
Centre National d'Etudes Spatiales, Toulouse, France

J. Bell
Arizona State University, Phoenix, AZ, USA

D. Cruikshank
NASA Ames, Moffett Field, CA, USA

J. Helbert
Deutschen Zentrums für Luft- und Raumfahrt, Berlin, Germany

F. Marzari
University of Padova, Padova, Italy

A. Morbidelli
Observatoire de la Cote d'Azur, Nice, France

P. Rosenblatt
Observatoire Royal de Belgique, Bruxelles, Belgium

H. Sierks
Max Planck Institute for Solar System Studies, Lindau, Germany

asteroids are small primitive bodies located beyond the 'snow line', around respectively the L_4 and L_5 Lagrange points of Jupiter at ~5.2 AU (Trojans) and in the 2:3 mean-motion resonance with Jupiter near 3.9 AU (Hildas). They are at the crux of several outstanding and still conflicting issues regarding the formation and evolution of the Solar System. They hold the potential to unlock the answers to fundamental questions about planetary migration, the late heavy bombardment, the formation of the Jovian system, the origin and evolution of trans-neptunian objects, and the delivery of water and organics to the inner planets. The proposed Trojans' Odyssey mission is envisioned as a reconnaissance, multiple flyby mission aimed at visiting several objects, typically five Trojans and one Hilda. It will attempt exploring both large and small objects and sampling those with any known differences in photometric properties. The orbital strategy consists in a direct trajectory to one of the Trojan swarms. By carefully choosing the aphelion of the orbit (typically 5.3 AU), the trajectory will offer a long arc in the swarm thus maximizing the number of flybys. Initial gravity assists from Venus and Earth will help reducing the cruise time as well as the ΔV needed for injection thus offering enough capacity to navigate among Trojans. This solution further opens the unique possibility to flyby a Hilda asteroid when leaving the Trojan swarm. During the cruise phase, a Main Belt Asteroid could be targeted if requiring a modest ΔV. The specific science objectives of the mission will be best achieved with a payload that will perform high-resolution panchromatic and multispectral imaging, thermal-infrared imaging/ radiometry, near- and mid-infrared spectroscopy, and radio science/mass determination. The total mass of the payload amounts to 50 kg (including margins). The spacecraft is in the class of Mars-Express or a down-scaled version of Jupiter Ganymede Orbiter. It will have a dry mass of 1200 kg, a total mass at launch of 3070 kg and a ΔV capability of 700 m/s (after having reached the first Trojan) and can be launched by a Soyuz rocket. The mission operations concept (ground segment) and science operations are typical of a planetary mission as successfully implemented by ESA during, for instance, the recent flybys of Main Belt asteroids Steins and Lutetia.

Keywords Asteroids · Trojans · Space mission · Solar system

1 Introduction

In our present understanding of the Solar System, small bodies (asteroids, Jupiter Trojans, comets and TNOs) are the most direct remnants of the original building blocks that formed the planets. As such, they contain a relatively pristine record of the initial conditions that prevailed in our solar nebula some 4.6 Gyr ago. In this regard, their physical nature, distribution, formation, and evolution are fundamental to our understanding of how planet formation occurred and, ultimately, why life exists on Earth. In fact, even though small

bodies represent only a tiny fraction of the total mass of the planets, their large numbers, diverse compositions, and orbital distributions provide powerful constraints on planet-formation models.

Jupiter Trojan and Hilda asteroids are small primitive bodies located beyond the 'snow line', around respectively the L_4 and L_5 Lagrange points of Jupiter at ~5.2 AU (Trojans) and in the 2:3 mean-motion resonance with Jupiter near 3.9 AU (Hildas). They range in size from a few meters to a few hundreds of kilometers and their total number is believed to be comparable or even exceed that of the Main Belt asteroids. Their origin—still unknown—remains a major challenge to present theories of the formation of the Solar System. There are two current scenarios, each one having distinct implications for the origin and early dynamical evolution of the Solar System.

The first model proposes that the Trojans and a large fraction of the Hildas originally formed where they are seen today—with the Trojans being captured onto their current orbits while Jupiter was growing.

An alternative model (the so-called Nice model [1–3]) suggests that a large fraction of both the Trojans and the Hildas has formed in more distant regions—typically in the primordial trans-neptunian disk, which is also the precursor of the Kuiper belt—and subsequently chaotically migrated towards the inner Solar System during the time when all four giant planets migrated, before being trapped at their current location. The radial migration of the giant planets is believed to be the last major event that sculpted the structure of the Solar System.

A mission to the Trojans and Hildas could constrain their origin, and in turn contribute to validate one of the two models or even call for a new scenario. This would have profound effects on our understanding of the early Solar System history and processes, including planets migration, the late heavy bombardment and large-scale transport.

Up to now, no mission has gone through the regions in space where Hildas and Jupiter Trojans are located while all major populations of objects in our Solar System have been visited by spacecraft, or are in the process of being encountered by on going missions (e.g., the New Horizons Pluto/KBO mission). A mission to these objects would thus allow the exploration of the last major—yet unexplored—populations of primitive bodies and contribute to answering the following key questions about the early history of the Solar System:

> Did they originate near Jupiter's orbit or farther out in the Solar System? Are they the building blocks of the giant planet cores or instead more accessible Kuiper Belt Objects?
> What do compositions of these primitive bodies tell us about the region(s) of the solar nebula in which they formed? How much compositional variability is there among them?
> Is there any evidence of life precursors in the form of simple organics and water ice on these bodies? Are they volatile-rich or volatile-poor?

What is the mineralogy of the silicates in these objects? To which extent did radial mixing of protoplanetary dust occur during the early phase of the Solar System formation?
How do the geological processes that have occurred on both Trojans and Hildas compare to those that have affected other small bodies? Are they homogeneous or differentiated?
How are the properties of Trojan and Hilda surfaces modified over time by the space environment?
What are the main impactor populations in these regions of the Solar System?
How diverse are these objects?
How do they compare to comets, TNOs, outer planet satellites, and Main Belt asteroids?

2 Scientific objectives and requirements

2.1 Science goal and overview

The overarching science goal of the proposed Trojans' Odyssey mission is to explore the Jupiter Trojans and Hilda asteroids in order to unveil the early history of the Solar System. These objects are at the crux of several outstanding and still conflicting issues regarding the formation and evolution of the Solar System. They hold the potential to unlock the answers to fundamental questions about planetary migration, the late heavy bombardment, the formation of the Jovian system, the origin and evolution of trans-neptunian objects, and the delivery of water and organics to the inner planets. This overarching goal has been formulated in a series of questions presented in the introduction from which we derive below the primary science objectives of the mission which directly address two of the four key scientific questions highlighted in ESA's Cosmic Vision program:

What are the conditions for planet formation and the emergence of life?
How does the Solar System work?

The mission would achieve its science objectives with a payload that will perform high-resolution multispectral imaging, thermal-IR radiometry, near-IR and mid-IR spectroscopy, and radio science/mass determination.

2.2 Mission and target requirements

The proposed Trojans' Odyssey mission is envisioned as a reconnaissance mission fulfilling the high level requirement of probing the diversity of the Jupiter Trojans and Hildas.

The mission should therefore aim at visiting several objects, typically five Trojans and one Hilda. Although this can be achieved by combining an orbital exploration and subsequent flybys, a strategy adopted by the Odysseus

proposal submitted to NASA in 2008, the technical implications would raise the cost beyond the current limit imposed by ESA in the present AO. Our science goals can perfectly be met by a multiple flyby mission, which remains within the ESA financial constraints of a M-class mission.

The mission will attempt exploring both large and small objects and sampling those with any known differences in photometric properties. As far as possible, it will focus on: (a) the never-disrupted objects with diameters larger than 80–90 km (typically, 1 to 2 objects), and collisional fragments with diameters under 80–90 km (typically, 3 to 4 objects), and (b) sampling objects with differences in albedos ("dark" objects with albedo $\sim$0.05, and "bright" objects with albedo $>$0.15).

For the collisional fragments, we will attempt visiting objects belonging to well-defined families, in order to probe the interior of the parent body and to search for volatiles on their surfaces as expected in the framework of the Nice model. For the largest objects, priority will be given to binary objects.

Last, the exploration of the diversity of the Trojans would be slightly better achieved by visiting the L_4 cloud instead of L_5. Currently, the diversity in terms of albedos and spectral classes is broader in L_4 than in L_5 (note that this may change when more data will be collected by forthcoming surveys).

2.3 Science objectives

We now describe our specific scientific objectives and identify the data sets needed for each objective. When appropriate, we specify how the measurements to be performed by the Trojans' odyssey mission will directly contribute to answering ESA's Cosmic Vision (CV) program.

2.3.1 Determine the physical parameters

The global physical parameters of an object, essentially shape and size, already contain significant information on its formation and subsequent evolution. A spheroidal shape tend to suggest a monolith body while an elongated one suggests the coalescence of two (or more) components which in turn may have different properties. Very irregular bodies suggest collisional shards. Specific shapes are very instructive. For small objects ($D < 20$ km), a 'spinning top' shape gives strong constraints on the efficiency of the YORP effect in shaping their appearance. Likewise binary systems imply specific conditions for their formation. The shape of Hektor, the largest Trojan, is presently best approximated by a Roche contact binary model, which constrains its density to 2.5 g/cm^3 [4]. Otherwise, the determination of the bulk density requires, beside the mass, the volume of the body which in turn requires an accurate size determination and shape model.

To achieve this first objective, we need to acquire global images at a spatial resolution greater than 1% of the target's size and to achieve the largest surface coverage. We further need light curves at various aspect angles obtained by the spacecraft during the approach phase and by supporting ground-based

observations (with a relative photometric accuracy of a few percents) to constrain the part of the volume not seen by the spacecraft.

2.3.2 Determine the photometric properties

Likewise, global photometric properties already contain significant information and constitute the basic parameters for the classification of minor bodies. We will derive these global properties for each target, namely the geometric and Bond albedos, the phase function, the broadband colors and the spectral reflectivity. To achieve this objective, we need to acquire photometric measurements over both a broad range of phase angles (0–50°) and a broad spectral range with a relative photometric accuracy <3% and an absolute accuracy <10%.

Spatially resolved photometric properties of the surface are of paramount importance to tackle questions such as geologic formations and terrains, regolith evolution and space weather effects. They also provide an initial constraint of the surface composition. This requires obtaining multiple spectral images at different phase angles during closest approach and at spatial resolution of typically ~50 m and photometric accuracy <10%. We will derive reflectivity maps (often improperly called "albedo" maps). By combining with the shape model, we will determine the local photometric properties of each facet of the model (for instance, the Hapke parameters).

2.3.3 Determine the thermo-physical parameters

The spatial and temporal variations of temperature on the surface result from the local topography, the physical properties of the surface materials (albedo, emissivity, roughness, thermal inertia), the composition of the surface (silicates or volatile materials), and the physical processes involved in the surface energy balance (thermal emission, conductivity, sublimation of volatile materials, exothermic processes).

The temporal variations of the surface temperature as a function of rotation (diurnal changes) are characteristic of the thermal inertia, which connects to several physical properties: the heat conductivity, the heat capacity, and the density. The thermal inertia also provides information on the nature and distribution of regolith on the surface, which is a key point to understand the surface history; the lower the thermal inertia, the finer and thicker is the regolith. From the thermal inertia, we can also estimate to which depth the energy of the Sun penetrates into the target, and then to which extent it is still primordial or evolved. While the thermal inertia is accessible via remote, disk-integrated, mid-IR observations from the ground, its meaning with respect to the surface properties and morphologies can only be achieved by in-situ observations.

The temperature is also crucial to identify the main physical process involved in the surface energy balance, and to discriminate between surface and sub-surface processes, e.g., for the sublimation of volatile materials if they are present.

Finally, in combination with spectroscopic data in the mid-infrared that can provide information on the emissivity, it is possible to derive the surface roughness from the temperature maps. Roughness provides information on the nature and mechanical properties of the surface materials, which are of particular interest to properly interpret the geological features visible on the surface (slopes, cracks, pits, erosion).

To properly investigate the thermal properties of the objects' surfaces, we need to obtain temperature maps at spatial resolution better than 3% of the target's size and with an accuracy of ∼2 K.

2.3.4 Characterize the geology of the surface and the regolith properties

Due to the unknown nature of Trojans and Hildas surfaces, it is unclear whether rocky asteroids or icy outer Solar System bodies provide the proper analogs. In principle, these two types lead to very different geological features thus helping in answering the question. However we may face a more complex situation with a mix of the two types as illustrated by the nucleus of comet 9P/Tempel 1: a prominently rocky surface with limited patches of water ice rich material. The analysis of geological formations at all possible spatial scales will be crucial for deciphering the nature of our targets: smooth plateaus, cliffs, hills, grooves. Tectonic features such as fault planes and cracks may be present, especially on the larger bodies, and will also be sought for.

It is however possible that a fraction of Trojans and Hildas are prominently covered by impact-derived regolith. The coverage, thickness, and maturity of the regolith layer mark the history of impacts and regolith distribution processes. Regolith properties can be assessed through small crater morphology, size distribution of ejecta blocks, and the identification of local slopes subject to regolith mass movement. Regolith movements can be revealed by the formation of smooth, gravitationally controlled pond-like deposits in craters, and landslides as illustrated by asteroids Lutetia (Fig. 1) and Eros (Fig. 2).

Craters are a special case of geologic formations. They reveal such a vast amount of information that we address here their relevance to the physical properties of the surface material, leaving other aspects to the section below. For objects with similar surface gravity (asteroids, Jupiter Trojans, Saturnian satellites), differences in crater morphology (e.g. depth-to-diameter ratio) can be attributed to compositional or rheological differences. Inter comparison between the crater morphology on rocky asteroids, icy Saturnian satellites and Jupiter Trojans may therefore help deciphering the nature of the terrains. The morphology of small craters can help constraining the properties of the regolith. Larger craters may uncover distinct layers or even a bedrock thus giving access to the subsurface structure. Finally, it will be of utmost interest to investigate whether there are significant differences between the geology of large and small Trojans in connection with their suspected different evolutions.

To achieve these objectives, we need to acquire images in a broad range of spatial scales, from the overall body to give the global context and map

Fig. 1 Crater on Lutetia, imaged by Rosetta. (Credit: ESA/OSIRIS team)

global pattern, to the highest possible spatial resolution that will be achieved at closest approach (and which depends upon the geometric circumstances of the encounter). Topography at a scale of typically 50 m (as achieved by the NAC camera during the recent flyby of Lutetia) will be derived from multiple "stereo" images using the techniques of stereo-photogrammetry and stereo-photoclinometry. Determining local slopes is indeed crucial to understand regolith mass movement and to refine the morphology of craters and other geologic features such as knobs, ridges, and flows whose shapes provide insight into surface geology and subsurface structure.

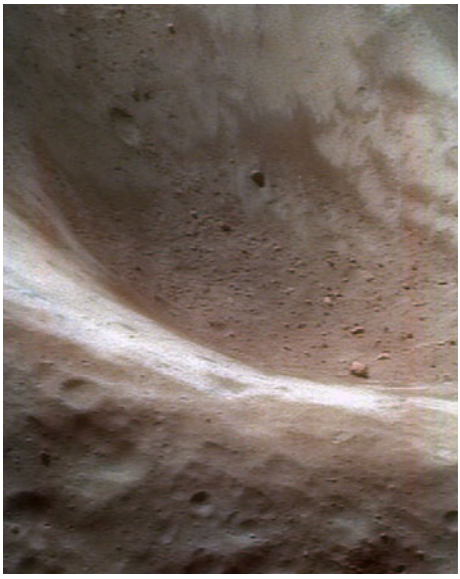

Fig. 2 Crater on Eros, imaged by NEAR-Shoemaker. (Credit: NASA/JPL/JHUAPL)

2.3.5 Characterize the collisional history, the collisional environment and determine the age of the objects

Craters at the surface of Solar System bodies provide a valuable record of the bombardment history and of the collisional environment. Both kinds of information in turn, help constraining the object's surface age (the surface age refers to the date of the last disruption event of an object and/or the last resurfacing event).

On 'old' surfaces with very low weathering rates or other crater erasure mechanisms (typically the case for Jupiter Trojans and Hilda asteroids), the size–frequency distribution of impact craters follows the shape of the impactor population that produced it. Once the main impactor population has been identified, one can determine the expected collisional rate in that region of the Solar System and finally constrain the age of the surface. Whenever possible, we will compare the surface age of the two suspected populations of Trojans, undisrupted objects versus collisional fragments.

The data sets needed to achieve this goal are similar to those listed in the previous section.

2.3.6 Characterize the composition of these primitive bodies and look for evidences of life precursors in the form of simple organics and water ice on these bodies

We will determine the mineralogy of the silicates likely to be present at the surface of the objects. Silicates—olivines and pyroxenes in particular—are ubiquitous throughout the Solar System, from Mercury to comets. For both silicate groups, formations at different temperatures (i.e. different distances from the Sun) result in different spectral properties and compositions. Constraining their composition will give us insights on the chemistry of the building blocks of both the giant planets' and their satellites' cores (in the case of the classical model) or gives us constraints on the radial mixing process of dust in the early Solar System if one assumes the Nice model to be correct.

Large silicate grains ($>$10–15 μm) of pyroxene and olivine will be searched for via the presence of broad absorption bands at $\sim$1 and $\sim$2 μm (finding them will depend on their exposure in a spatial sense, since the disk-integrated spectra obtained from Earth do not show specific absorption bands attributed to these minerals).

The composition of fine-grained silicates ($<$5 μm) will be investigated in the 7–14 μm spectral domain where they have a strong emission peak (around 10 μm). Importantly, this spectral region also allows determining if the silicates are mainly crystalline or amorphous.

We will also search for water ice and organics on the objects' surfaces. These compounds have been uncovered on the surfaces of airless moons, comets and Kuiper belt objects; more elaborate organics are found within carbonaceous chondrites. By analogy with life as known on Earth, it is generally believed that primitive life-forms developed from the processing of reduced organic

molecules by liquid water. Generally, liquid water is considered to be one of the pre-requisites for life in that it would have to be present on a terrestrial planet for life to develop.

Although it is well understood that volatiles (organics and water) were captured during and following the accretionary and "late heavy bombardment" stages of Earth evolution, their origin remains one of the most important subjects in the field of Solar System formation. On the one hand and according to the nebular model of Drouart et al. [5], the Jupiter–Saturn region and the outer asteroid belt (exactly the regions where Trojans and Hildas are seen today) should be the only regions where planetesimals could have included water with essentially the isotopic composition of the Earth. On the other hand, objects that formed beyond Neptune's orbit contributed at most 10% to the Earth's water budget [6]. Applied to Trojans and Hildas, this implies that we will either visit the only surviving planetesimals from the Earth's main volatile source region (classical model) or a minor contributing population to the Earth's water budget (Nice model).

It is highly unlikely that other ices could be present at the surface of Trojans and Hildas. While CO_2 has been identified by its asymmetric stretching mode band near 4.27 μm on several Jupiter and Saturn moons, it does not occur as a pure ice, but as a molecular complex mixed with other materials.

Near-infrared spectroscopy is the ideal tool for detecting the presence of (a) water ice and/or (b) hydrated minerals, and (c) organics on a planetary surface.

(a) The spectrum of water ice shows absorption bands at 1.5, 1.65 (only crystalline water ice), 2.0, and 3.0 μm, the latter one being the deepest (Fig. 3).
(b) Minerals with water molecules either absorbed or in their crystal structure exhibit relatively well defined absorptions in their spectra near 1.4, 1.9 and 3 μm as well as overtones (minor bands) in the 2.1–2.5 μm region. The precise position and shape of the hydration bands vary with composition allowing distinguishing, for example, between the presence of sulfates or phyllosilicates on the observed surface. The latter distinction, in turn, gives strong constraints on the aqueous alteration history of the parent body.
(c) The presence of organics, aromatic and aliphatic hydrocarbons, can be detected via the C–H stretching mode occurring at 3.29 μm in aromatic hydrocarbons and at 3.40–3.55 μm in aliphatic hydrocarbons.

Independently of the to-be discovered diversity among Trojans and Hildas, the detection or not of water on their surfaces (as ice or simple hydration) might, in principle, tell us whether they formed close to Jupiter or in the Kuiper Belt (Classical model versus Nice model).

For the classical model to be correct, the detection of water on the Trojan surfaces currently appears as a prerequisite. The systematic detection of water on the Galilean (apart from Io) and Saturnian satellites makes water a primary

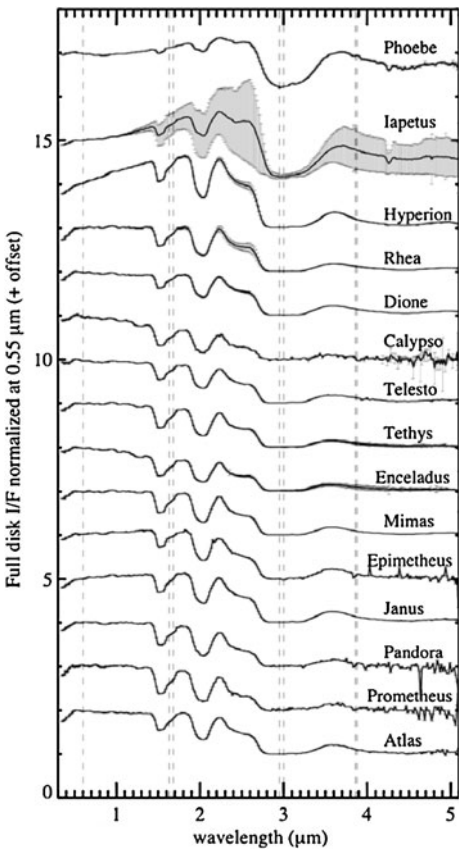

Fig. 3 VIS–NIR full-disk mean reflectance spectra of the saturnian satellites. Vertical lines indicate the spectral ranges of the instrument filters, one in the VIS and three in the IR ranges [9]

tracer for a local formation scenario in this region of the Solar System. Note that water may be observed on the Trojan's surface as ice (like on Ganymede, Europa, Callisto and the Saturnian satellites, see [7]) or as simple hydration feature [8].

For the Nice model to be correct, most of the Jupiter Trojans and Hildas should resemble featureless dormant/extinct comets since their surfaces are supposed to have been largely devolatilized prior to their capture (in the Lagrange points or in the 3:2 resonance) by Jupiter.

Mid-infrared spectroscopy can provide complementary compositional information that is not accessible in other spectral domains. Indeed, certain major mineral groups that lack useful diagnostic features at visible to near-IR wavelengths do produce diagnostic mid-infrared features. This is exactly the case for the Jupiter Trojans whose mid-infrared spectra show the most pronounced emissivity features observed so far on asteroids [10, 11].

To achieve the above objectives, we need spectral data at moderate spatial resolution (5% of the target size) and moderate spectral resolution.

2.3.7 Search for evidence of surface space weathering

Continuous irradiation of the surfaces of small bodies by solar wind particles and/or micrometeorites (so-called space weathering) progressively modifies their initial properties. In the case of silicate-rich surfaces, the observed effect is a darkening of the surface (lower albedo) and a reddening of the reflectance spectrum. In the case of ice-rich surfaces, laboratory experiments simulating the solar wind bombardment (via ion irradiation) predict the formation of an organic refractory residue [12]. The presence of such an irradiation mantle could spectrally mask the pristine molecules underneath, such as water.

High-resolution spatial imaging and spectroscopy of the objects' surfaces will allow us characterizing the regolith alteration. Images will, in a first step, help us distinguishing young regions from older ones (via crater counts) and, in a second step, allow us to measure the spatially resolved photometric properties (albedo) for surfaces of different ages. In turn, the "albedo" maps derived from high-resolution images will provide a context for the spectral data to be obtained by both the NIR and MIR spectrometers so that the spectral effects induced by space weathering processes can be fully investigated over a large wavelength domain.

2.3.8 Search for evidence of activity

The question of the presence of volatiles in Trojans and Hildas is ultimately tied to the question of outgassing activity, either past or present and either continuous or transient. If indeed these objects contain significant amount of ices, then past and possibly present activity should manifest itself by different signatures. Such activity affects the surface layer, and could express itself directly or indirectly in the geology by specific features such as smooth terrains, vents, fissures, flows, rays, etc [13]. Images at high spatial resolution for morphology and spectral reflectivity maps for albedo and color variations and spectral signatures will be analyzed to possibly identify both past and recent sites of volatile activity. Activity may also be detected by the presence of anomalies (cold or hot spots) in the surface temperature distribution derived from thermal imaging.

Regarding present activity, it can be revealed by the presence of a thin coma possibly structured by jets connected to active regions as observed in comets. The most appropriate technique for detecting such a coma relies on solar and stellar occultations in the ultraviolet, but this cannot be practically implemented in a flyby mission. A viable alternative consists in obtaining images at large phase angles, usually after closest approach as the spacecraft leaves the target. Light scattering by dust particles is enhanced and may reveal faint jets as in the case of comets Tempel 1 and more recently Hartley 2.

A very favorable case would be the recent impact that exposes deep icy layers thus leading to transient activity and the production of a weak coma. Such impact events are not uncommon and one has recently been observed in

the Main Belt. Its detection by the OSIRIS/NAC aboard Rosetta attests to the capability of this kind of imager to reveal extremely faint activity [14].

2.3.9 Probe the internal structure and composition

Bulk density is a key parameter to characterize composition and internal structure. In the case of pure rocky bodies such as Main Belt asteroids, the density of the body is compared to that of the associated meteorites and any difference is attributed to internal porosity, which is therefore quantified. Generally a large porosity is connected to a "rubble-pile" internal structure implying that the body coalesced from collisional fragments. The situation becomes more complex with icy bodies as the bulk density will reflect both composition (i.e., the rock-to-ice ratio) and internal porosity. Even if a "rubble-pile" structure is unlikely for Trojans and particularly the largest ones, the hydrostatic core pressure remains small and internal compaction is limited. Then internal structure will reflect a combination of composition, formation process and thermal and collisional history. Therefore proper interpretation of the density will require an assumption on the internal structure, which may be inferred from either Galilean and Saturnian satellites (classical model) or comets and TNOs (Nice model).

To clarify these questions, we need to determine bulk densities with an accuracy of $\sim$10%. This requires a determination of the volume as already addressed in the first objective and of the mass. Mass estimates can be obtained through spacecraft acceleration (Doppler shift of radio-frequency signal) during flyby. The feasibility and accuracy of these measurements are critically dependent on the mass of the body, the miss-distance and spacecraft parameters (size of antenna, power of transmitter) and will have to be analyzed on a case-to-case basis. Density can also be directly determined if a satellite is detected and this is addressed in a separate objective below.

More generally, the question of the internal structure can be addressed by different indirect methods. Very large craters penetrate very deep inside and their morphology (depth-to-diameter ratio, slope) can constrain the interior. Alternatively, members of a (collisional) family could give access to the interior of the parent body. Whatever formation scenario, the families were created when the parent body was already in one of the Lagrange swarms. It is therefore desirable that at least one target be a member of a family to search for differences with respect to non-members. This will be best addressed by NIR and MIR spectra as already described above.

2.3.10 Search for satellites

The presence of a satellite orbiting one or several targets would dramatically increase the scientific crop of the flyby. First, this offers the possibility to characterize an extra body, although probably not at the level of detail as the primary. Second, this allows directly determining the density of the primary.

Third, the putative presence of many companions will have to be explained (capture?) and will put constraints on the scenarios of formation and evolution.

We will therefore search for the presence of companions down to the limiting magnitude (V∼20) reachable by the imaging system and seek to determine its orbital parameters using multiple observations with different geometries.

2.3.11 Compare and contrast the properties of Trojans and Hildas between each others and with other minor bodies of the Solar System

The physical and chemical properties of the Trojans and Hildas visited by the mission will be compared to the properties of other families of small bodies in the Solar System: Near-Earth asteroids, Main Belt asteroids, comets, Centaurs, TNOs, Galilean satellites, and Saturnian satellites. This comparison will allow us to determine if both the Jupiter Trojans and Hildas form new, independent, populations or if they can be linked to already existing ones. We will particularly emphasize comparisons with small bodies already visited by spacecrafts. Finally, we will also search for similarities and differences within the Trojans themselves, to see if they form a homogeneous, as predicted by the classical model, or a heterogeneous population, as predicted by the Nice model.

The data set required to achieve this goal includes all the scientific results listed above.

2.4 Additional science: Main Belt asteroid

As the Trojans' Odyssey spacecraft will cross the Main Belt of asteroids, this offers the possibility to flyby an additional target at little extra cost as implemented on practically all deep-space missions. The bonus science will complement our growing database of Main Belt asteroids. The flyby itself will offer an opportunity for practice and calibration exercise in preparation of the Trojans' flybys.

3 Mission baseline

The exploration of the Trojan and Hilda asteroids and their diversity, and the reconnaissance aspect of the mission will be best achieved by visiting typically five Trojans and one Hilda. The proposed strategy consists in a direct trajectory to one of the Trojan swarm. By carefully choosing the aphelion of the orbit (typically 5.3 AU), the trajectory will offer a long arc in the swarm thus maximizing the number of flybys (Fig. 4). Initial gravity assists from Venus and Earth will help reducing the cruise to less than 10 years as well as the ΔV needed for injection thus offering enough capacity to navigate among Trojans. This solution further opens the unique possibility to flyby a Hilda asteroid when leaving the Trojan swarm. During the cruise phase, a Main Belt Asteroid could be targeted if requiring a modest ΔV.

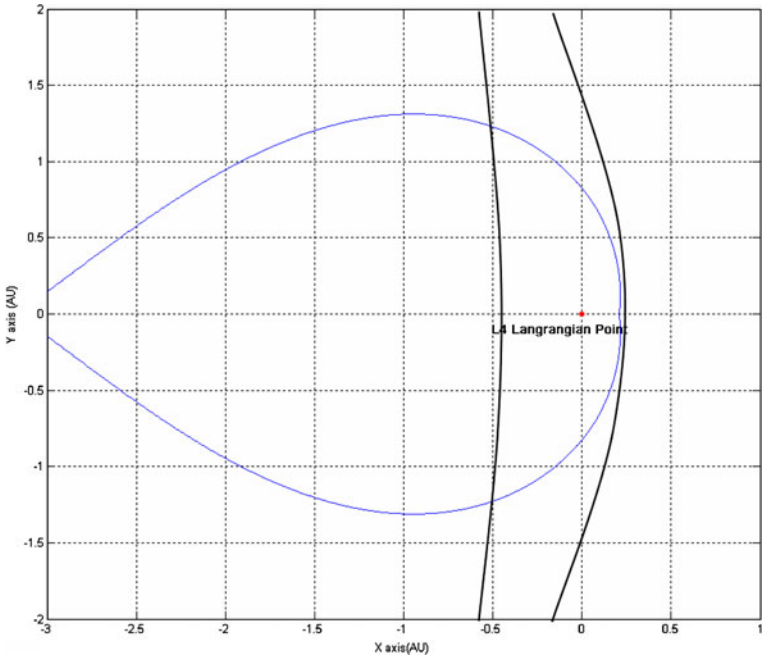

Fig. 4 The proposed "8-shaped" trajectory (in the L4 referential)

Table 1 Direct trajectories with flyby of five Trojan asteroids arriving in the L4 swarm in 2029

ast1	ast2	ast3	ast4	ast5	Δv_{tot}	Date of last fly-by
2009UC87	2009WD2	2009SJ48	2009SA354	Balios	1399	31/12/2030
2002EN48	2004HR57	2002EH157	2008RV123	2010OX110	1332.5	21/10/2031

Table 2 Detail of the two direct trajectories with the different gravity assists and the five flybys

	Date	Δv (m/s)		Date	Δv (m/s)
Earth	21/05/2023	–	Earth	22/05/2023	–
Venus	11/09/2023	54	Venus	11/09/2023	56.5
Earth	07/01/2025	–	Earth	07/01/2025	–
DSM	05/07/2025	35	DSM	15/09/2025	36
Earth	07/01/2027	–	Earth	07/01/2027	–
DSM	06/08/2027	588	DSM	23/10/2027	366
2009UC87	06/08/2029	293	2002EN48	06/04/2029	140
2009WD2	29/11/2029	104	2004HR57	26/07/2029	59
2009SJ48	01/06/2030	192	2002EH157	29/05/2030	320
2009SA354	07/10/2030	133	2008RV123	13/08/2030	355
Balios	31/12/2030	–	2010OX110	21/10/2031	–
Total duration	7.6 years		Total duration	8.5 years	
Arrival to 1st asteroid		677	Arrival to 1st asteroid		458.5
Δv for flybys		722	Δv for flybys		874

A recent orbital study has developed a complete methodology for the design of trajectories with visits to several Trojan asteroids and validated the proposed solution of multiple flybys [15]. Based on the 3000 currently known asteroids in the L4 cloud, this simulation shows that there are 36 trajectories that achieve 4 flybys and 2 that achieve 5 flybys, all with flyby velocities in the range 5 to 6 km/sec. For example, we present the latter solutions, which assume a launch date in May 2023. Table 1 lists the targeted Trojan asteroids

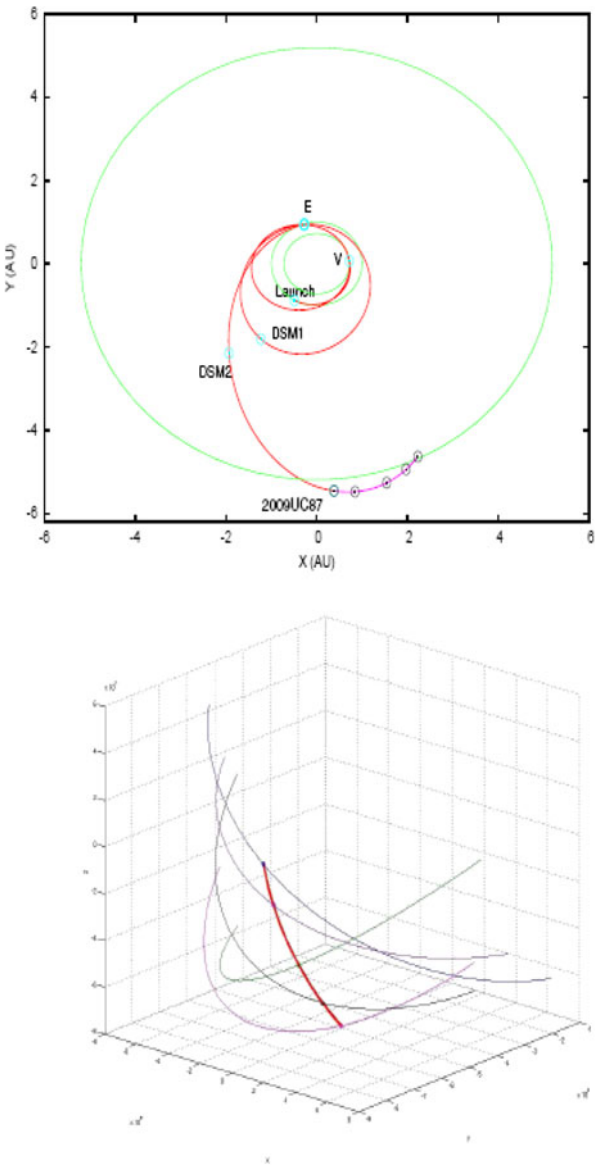

Fig. 5 Two views of the direct trajectory with launch in 2023 and including visits to five Trojan asteroids (see Tables 1 and 2). *Top* ecliptic heliocentric view. *Bottom* three-dimensional detail of the trajectory when it crosses the swarm, including the predicted orbits of the five asteroids for a period of two years centred at the time of their flyby. The X- and Y-axis have units of 10^8 km while the vertical Z-axis has units of 10^7 km

and the total ΔV needed in both cases. Table 2 gives the chronology of the two trajectories with the different gravity assists, deep space maneuvers (DSM), total durations of respectively 7.6 and 8.5 years and ΔV budgets. Figure 5 illustrates the trajectory corresponding to the first solution (left panel of Table 2).

The final choice of the targets will be investigated during the definition phase and will result from a trade-off between launch window opportunities, available spacecraft resources and science return. Based on present studies, total mission duration of less than ∼9 years is anticipated.

The specific science objectives of the mission will be best achieved with a payload that will perform high-resolution panchromatic and multispectral imaging, thermal-infrared imaging/ radiometry, near- and mid-infrared spectroscopy, and radio science/mass determination. The total mass of the payload amounts to 50 kg (including margins) and its total ROM cost is estimated at 39.5 M€.

The spacecraft is in the class of Mars-Express or a down-scaled version of Jupiter Ganymede Orbiter. It will have a dry mass of 1200 kg, a total mass at launch of 3070 kg and a ΔV capability of 700 m/s (after having reached the first Trojan) and can be launched by a Soyuz rocket.

The mission operations concept (ground segment) and science operations are typical of a planetary mission as successfully implemented by ESA during, for instance, the recent flybys of Main Belt asteroids Steins and Lutetia.

4 Proposed model payload to achieve the science objectives

4.1 Overview of all proposed payload elements

The proposed suite of instruments constituting the science payload of the Trojans' Odyssey mission are classically those of a reconnaissance mission to small Solar System objects but optimized to the case of the flyby of asteroids located at about 5 AU. It incorporates remote sensing instruments (imagers and imaging spectrographs) and a radio science experiment. All remote sensing instruments will be co-aligned and body-mounted on the spacecraft. Following the successful approach implemented on Rosetta, the S/C will perform attitude control so as to point the instruments to the targets and perform scanning as appropriate.

Imaging will be performed by three instruments operating in two broad spectral domains, the visible (slightly extended to near the ultra-violet and near-infrared) and the mid-infrared.

- The Multicolor Camera and Near-infrared Spectrograph (MCNS) includes a visible multicolor imager (VIMI) acting as a framing camera with a pixel field-of-view (IFOV) of 18.8 μrad and a FOV of 2.2°. It operates in seven broad spectral bands extending from 250 to 850 nm (plus a clear filter);
- The High Resolution Panchromatic Camera (HRPC) offers the highest spatial resolution of the suite thanks to its IFOV of 5.4 μrad, a factor of

3.5 compared to VIMI. It has a FOV of 1.23° and operates in a single panchromatic band that extends from 450 to 850 nm;
- The Thermal Imager (THERMAP) performs imaging in a single broad band 7–18 μm. It is characterized by an IFOV of 100 μrad and a FOV of 3.7° × 2.75°.

Particular attention is paid to the performances of the visible imaging instruments so that, in addition to their specific science objectives, they can also serve for the navigation and pointing of the spacecraft.

Imaging spectroscopy will be performed by two instruments in two broad spectral domains, near-infrared and mid-infrared.

- The NIR spectrograph channel (NIIS) of the MCNS operates in the 0.9–3.6 μm range with a spectral sampling of 10 nm;
- The thermal imaging spectrometer TROTIS operates in the 7–14 μm range with a spectral sampling of 100 nm. In addition, TROTIS performs radiometric measurements in the 7–40 μm spectral range.

The Radio Science Investigation (RSI) consists in an X-band coherent transponder to measure the Doppler shift on a 2-way radio-link between the spacecraft and Earth-based tracking stations.

Table 3 summarizes instruments key resources and characteristics, relevant requirements, operating modes, current heritage and Technology Readiness Level (TRL). It is proposed that all instruments be procured by scientific institutes or consortia of institutes.

4.1.1 The Multicolor Camera and Near-infrared Spectrograph (MCNS)

The MCNS combines a visible multicolor imager (VIMI) framing camera and a near-infrared imaging spectrometer (NIIS) in a single mechanical unit body-mounted to the spacecraft. In a broad stroke, it replicates the OSIRIS Narrow Angle Camera of the Rosetta mission, but with an added NIR spectrograph as it was originally conceived [16]. The main scientific objectives of MCNS are to provide detailed information on the physical properties, the surface geology and the composition of the flyby targets.

The specific science goals of MCNS are:

- Determine the global physical properties of the objects: 3D shape, volume, rotational state
- Determine the topography of the objects
- Map the overall surface of the objects at high spatial resolution in several broad bands spanning the visible domain
- Determine photometric properties (geometric and Bond albedos, phase function) in the 250–850 nm spectral range
- Map the composition at medium spatial resolution
- Identify mineral, icy and organic material
- Detect possible activity
- Search for satellites

Table 3 Trojans' Odyssey instrument parameters

Instrument parameters		MCNS	HRPC	THERMAP	TROTIS	RSI
General information	Instrument type	VIS camera+ NIR imaging spectrometer	Visible camera	MIR camera (thermal)	MIR imaging spectrometer + radiometer	Transponder
	Sensor type	CCD array + HgCdTe array	APS array	HgCdTe array	HgCdTe array	–
	Heritage	Rosetta/ OSIRIS	New Horizon/ LORRI	BepiColombo/ Mertis	BepiColombo/ Mertis	Exo Mars/ LaRa
	System TRL	9	9	4	5	5.5
Physical specifications	*Mass*	22	8	5	6.5	0.75
	Baseline (kg)					
	Margin (%)	20	20	20	10	5
	Total (kg)	26.4	9.6	6	7.2	0.8
	Dimensions (mm)	320 × 650 × 765	200 × 200 × 600	200 × 250 × 325	200 × 250 × 325	154 × 130 × 45
	Co-alignment	Reference	1 arcmin	5 arcmin	20 arcmin	–
	Peak power consumption (W)	25	8	5	35	20
Operating conditions	IFOV (μrad)	18.8	5.3	100	135	–
	FOV (°)	2.2	1.2	3.7 × 2.75	2.0	–
	Sensor size (pixel)	VIS: 2k × 2k NIR: 270 × 438	4k × 4k	640 × 480	256 (spatial) ×128 (spectral)	–
	Working distance	1 AU	1 AU	10^5 km	10^5 km	10^4 km
	Spectral range	250–850 nm 0.9–3.6 μm	450–850 nm	7–18 μm	Spectro: 7–14 μm, Radiometry: 7–40 μm	–
	Spectral resolution (nm)	VIS: 50–80 nm NIR: 20 nm	–	–	200	–
	Spatial scale at 3500 km	66 m/pixel	19 m/pixel	350 m/pixel	470 m/pixel	–
Pointing requirements	Knowledge (°)	0.005	0.002	0.015	0.02	–
	Accuracy (°)	$6\ 10^{-3}$	$2\ 10^{-3}$	$2.8\ 10^{-3}$	–	–
	Stability/Jitter (°)	–	$8\ 10^{-5}$	–	–	–
Data volume	Gbytes/flyby	2	0.6	0.05	0.35	–
	Gbytes/Mission	14	4.2	0.35	2.45	–

The concept of combining imaging and spectroscopy was already present in the original design of the OSIRIS-NAC as noted above and is implemented on the HRI and RALPH instruments of respectively the Deep Impact and New Horizon missions, both still in flight operation. The two channels share the same telescope in a single package; a dichroic beamsplitter transmits near-IR wavelengths longer than 0.9 μm to NIIS and reflects shorter wavelengths to VIMI (Fig. 6). The telescope and framing visible camera nearly replicates the actual OSIRIS-NAC. The NIIS channel relies on the original NAC design [16] and also capitalizes on the heritage of similar channels of Rosetta/VIRTIS and its offspring of the Venus-Express mission, but an alternative concept implemented on Deep Impact/HRI could be considered (see detail below). Subsystems such as the filter wheel capitalize on more recent developments and designs introduced in the DAWN framing camera.

The telescope is an un-obstructed, off-axis, all-silicon carbide Three Mirror Anastigmat (TMA) (Fig. 7). Such a design where silicon carbide is used for both the mirrors and the structure is athermal and therefore well suited to a deep space mission. With an aperture of 90 mm and a focal length of 720 mm, this telescope offers an excellent compromise between spatial resolution and sensitivity to extended sources (f/ 8).

Likewise the OSIRIS-NAC, VIMI uses a cooled 2k × 2k framing CCD detector with extended sensitivity down to 200 nm. This results in a FOV of 2.2° and an IFOV of 18.8 μrad. At a range of 3500 km, this corresponds to a pixel scale of 66 m. Passive cooling at 180 K will be achieved by an external radiator. VIMI is equipped with an eight-position filter wheel holding seven interference filters with typical FWHM of 50 to 80 nm and spanning the interval 250 to 850 nm. An additional clear filter defines a broad panchromatic channel similar to that of High Resolution Panchromatic Camera (see below) for redundancy. This channel also serves for the optical navigation of the S/C being capable of detecting a (solar type) star down to a limiting V magnitude

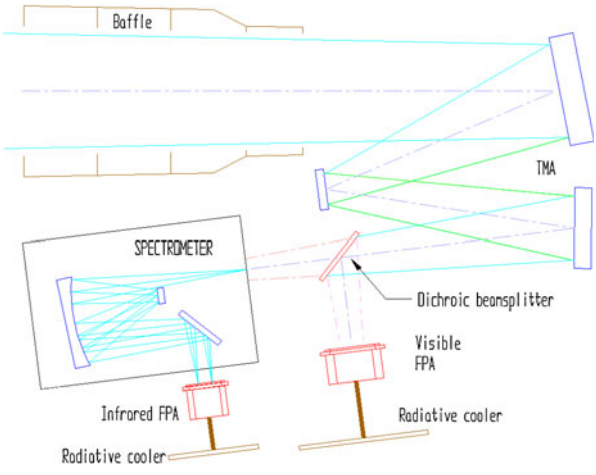

Fig. 6 Optical concept of the Multicolor Camera and Near-infrared Spectrograph

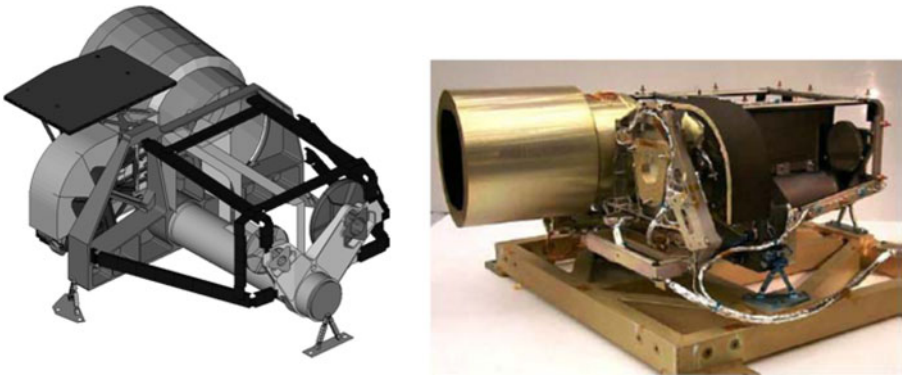

Fig. 7 Two views of the OSIRIS/NAC camera: a schematic showing the complete instrument (*left*) and the flight model (without the detector) presently aboard the Rosetta spacecraft (*right*). The proposed MCNS will be similar except for the adjunction of the near-infrared spectrograph

of 19.3 with a SNR of 5 in a 300 s exposure. Based on early observations of asteroid Steins performed in 2006 at a distance of 1.06 AU [17] and applying the appropriate scaling for heliocentric distance, size and albedo, it is readily shown that this "clear" channel can detect a 10 km diameter Trojan at a distance of 1 AU and at phase angle of 40° with a SNR of 10 using the same exposure time of 300 sec. For observations at close range, the corresponding exposure time will be ∼20 ms enabling to reach SNR > 100. VIMI will be operated as a framing camera with sub-framing and binning capabilities. It will continuously acquire images (with different filters as appropriate) during the flybys thus providing a complete record of the event. The miss-distance will be chosen so that the image of the object at closest approach remains within the FOV. Calibrations will be performed on-ground and in-flight using stars, planets and the Moon as available.

The near-infrared imaging spectrometer (NIIS) is conceived to cover the spectral range 0.9 to 3.6 μm so as to fulfil the science requirements. Its concept is based on the Offner spectrograph, which offers freedom from all third order aberrations along the slit as well as along the spectrum. This design is also very compact and has the additional advantage of physically separating the spectral image from the slit. It consists of two spherical reflecting surfaces with a common center of curvature (Fig. 6), the radius of curvature of the concave primary mirror being twice that of the convex grating. The slit, placed in the plane perpendicular to the optical axis and containing the center of curvature, forms a spectrum in the same plane after two reflections off the primary and a diffraction off the grating. With the aperture stop located at the grating, telecentricity is ensured in both object and image space. The slit is centred on the optical axis in the focal plane of the telescope and its width projects to 0.13 mrad on the sky. The spectral range extends from 0.9 to 3.6 μm and therefore extends over 2 octaves. Order sorting is required and accomplished by an appropriate filter placed just in front of the detector. Also in such a

grating spectrometer, the resolving power varies with the wavelength, from 90 to 360 in the present case. These shortcomings could be alleviated by using a prism spectrometer as implemented in the Deep Impact/HRI instrument [18] however resulting in a somewhat more bulky and optically complex system not favored in a first analysis. NIIS uses an optimized 270 × 438 pixels HgCdTe array with a pixel size of 38 μm, the spectral dispersion being oriented along the short side. The resulting spectral sampling amounts to 10 nm/pix. Along the slit, the FOV extends over 0.7°; this will allow covering 80% of a 100 km diameter Trojan at a flyby distance of 3500 km. The detector is passively cooled using an external radiator and further actively cooled to 80 K using a cryocooler. At this temperature, the dark current is typically 10 fA and the noise equivalent spectral radiance is of the order of 10^{-4} W/m^2/μm/sr at 2.5 μm. This typically translates to a SNR of 65 when observing a Trojan. Binning in spectral and, most certainly, in spatial directions can be performed by software mode to optimize the SNR. For instance, spatial binning by a factor 10 will result in a scale of 1.9 km at 3500 km, well in line with our science objectives. NIIS will operate in two modes. While on the incoming leg of the flyby trajectory and further imposing that (a) the target fills one half to one third of the FOV of VIMI for proper tracking, and (b) that the image scale varies by less than 10% during the whole sequence, scanning the slit over the nucleus of the comet is accomplished by rotation of the spacecraft, thus requiring that the axis of rotation be approximately perpendicular to the projected trajectory (±30° approximately). Typically 40 scans will be performed resulting in a spatial resolution of ∼1/40 of the object diameter. Upon completion of this sequence, the S/C will be constantly pointed to the center of the object and scanning across the surface of the object will naturally result from the rotation of the spacecraft. Calibrations will be performed on-ground and in-flight using stars, planets and the Moon as available.

A common DPU (Fig. 8) operates the whole instrument insuring the standard functions:

- Instrument control and monitoring
- Telecommand and telemetry handling (CCSDS packets via MIL-STD-1553B bus I/F)
- Acquisition of image/spectral data from detector readout electronics
- Mass storage of acquired image data to decouple image acquisition from image processing
- Housekeeping data acquisition (from MCU and PCU)
- Compression of image data
- On-board image processing
- Execution of observational sequences

4.1.2 The High Resolution Panchromatic Camera (HRPC)

The HRPC is a visible framing camera offering the highest spatial resolution of the payload suite. The main scientific objectives of HRPC are to provide

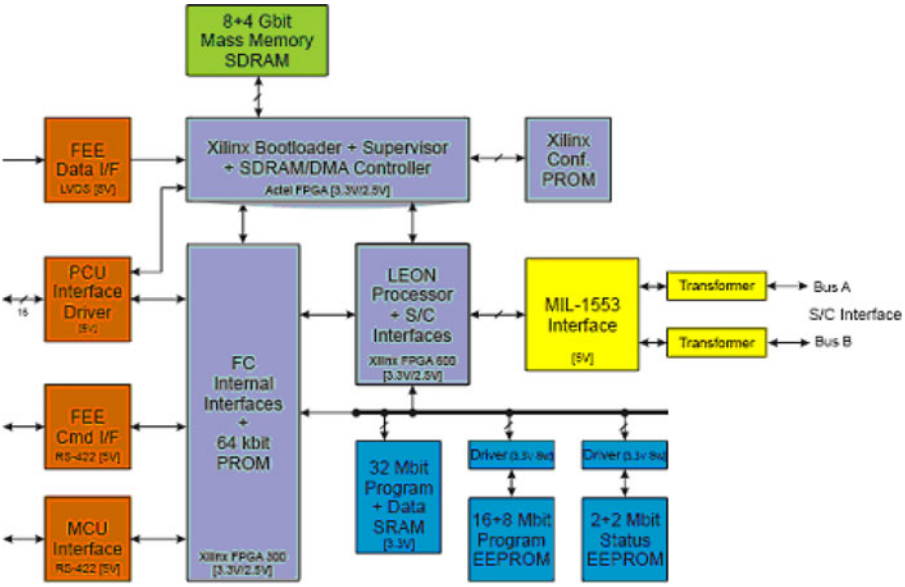

Fig. 8 Block diagram of the DPU of the Multicolor Camera and Near-infrared Spectrograph

the most detailed information on the surface of the Trojans and radiometric measurements in a broad, panchromatic spectral band 450–850 nm.

The specific science goals of HRPC are:

- Determine the global physical properties of the objects: 3D shape, volume, rotational state
- Determine the topography of the objects at high spatial resolution
- Determine broadband photometric properties (geometric and Bond albedos, phase function)
- Detect possible activity
- Search for satellites

Having such a high-resolution camera in parallel to a combined multicolor imager/NIR spectrometer follows the philosophy adopted in several planetary missions such as New Horizon (due to flyby Pluto and its satellites in 2015 and one or two Kuiper belt objects in 2018). In addition to obvious redundancy, it allows reaching a spatial resolution 3.5 times better than that of VIMI, or alternatively offers an ample margin should some flyby distances exceed our nominal values, therefore preserving several key science objectives.

The telescope of the HRPC is based on a classical Ritchey–Chrétien with a field-flattening triplet near the focal plane (Fig. 9) often implemented in past planetary mission, for instance on the VEGA mission to comet P/Halley. With an aperture diameter of 130 mm and a focal length of 1500 mm, it is further optimized for high system throughput by having a single broad band thus allowing short exposure times to limit possible smearing. Likewise the MCNS,

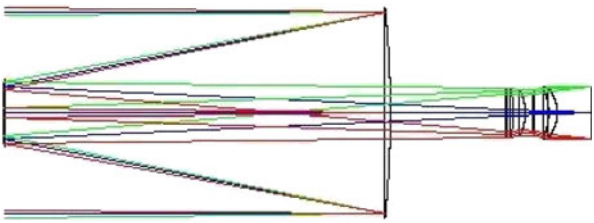

Fig. 9 Conceptual design of the HRPC telescope

the telescope has its two mirrors and structure fabricated from silicon carbide to realize an athermal system without the need for a re-focusing device. This is similar to the Long-Range Reconnaissance Imager (LORRI) of the New Horizon mission [19] (see Fig. 10). In essence, the HRPC telescope will be a down scale version of LORRI built on the same principle.

The HRPC uses a cooled 4k × 4k framing APS detector with a pixel size of 8 μm (such a detector is being developed for Solar Orbiter instruments). This results in a FOV of 1.22° and an IFOV of 5.3 μrad. At a range of 3500 km, this corresponds to a pixel scale of 19 m. Passive cooling will be achieved by an external radiator. No mechanical shutter is needed, this function being realized by the readout electronics. The HRPC has a single panchromatic band that extends from 450 to 850 nm (FWHM) and sensitivity to point-source comparable to that of VIMI with its clear filter. The HRPC can therefore serve for optical navigation as well. The sensitivity to extended source is somewhat inferior to that of the clear channel of VIMI, by approximately a factor 1.8. However the same exposure time of ∼20 ms at close range can be used since the SNR is still excellent (>55). The HRPC will be operated as a framing camera with sub-framing and binning capabilities in coordination with VIMI. In summary, the HRPC is designed as a very robust instrument with no mechanism, except for an aperture door. Its calibrations will be performed on-ground and in-flight using stars, planets and the Moon as available.

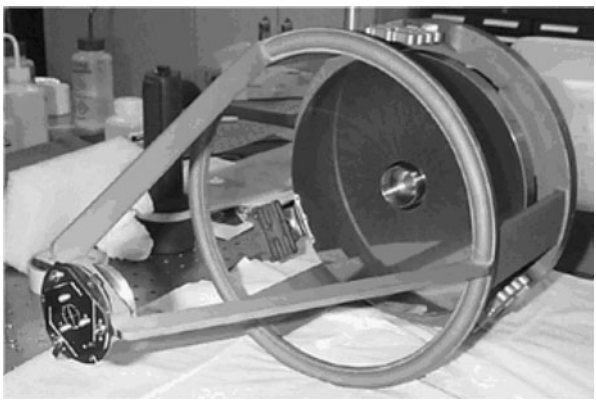

Fig. 10 The LORRI telescope flying on the New Horizon mission [19] showing the SiC mirrors and structure

The HRPC is operated by its own DPU whose architecture is similar to that of the MCNS but simplified due to the presence of only one detector and one mechanism.

4.1.3 The thermal mapper (THERMAP)

THERMAP is a thermal imaging instrument with high spatial resolution, complementary to the visible camera and to TROTIS. THERMAP observes the surface in the thermal infrared (7–18 μm) to derive its temperature. THERMAP provides thermal images of the entire surface with a spatial resolution >10 times better than the radiometric channel of TROTIS (see below).

The main scientific objectives of THERMAP are:

- Determine the temperature map of the entire surface at high spatial resolution (∼350 m per pixel at 3500 km)
- Constrain the surface and sub-surface physical processes
- Investigate any temperature anomalies (cold or hot spots) to identify local exothermic and endothermic processes (activity)
- Constrain the nature of the surface materials (depth of the regolith, presence of volatiles) and their physical properties (thermal inertia, roughness, mechanical properties)

The THERMAP instrument mainly has the heritage of MERTIS, the Mercury radiometer and thermal infrared spectrometer for the Bepi-Colombo mission [20], but has been adapted to measure colder temperature (typically 120–170 K for the surface of Trojans). Since THERMAP operates in the same wavelength range than TROTIS, the two instruments will be developed in parallel.

THERMAP uses a cooled HgCdTe detector (7–18 μm) with 640 × 480 pixels of 27 μm. The instrument is mounted on the instrument platform, passively cooled to 110 K. The detector is then cooled to 77 K using a cryocooler (pulse tube cooler). The heat is evacuated by a radiator, which is located on top of the instrument, towards deep space. The instrument integrates the thermal flux of the target between 7 and 18 μm, from which the temperature is derived. The expected sensitivity of the detector of about 5×10^{-4} W/m^2/μm/sr will allow to measure surface temperatures above 100 K with a SNR > 10, and above 130 K with a SNR > 100.

The optical design of THERMAP is based on a Three Mirror Anastigmat (Fig. 11) with a 270 mm focal, f/ 2.7 (i.e., an aperture of 100 mm), a total field of view of 3.7° × 2.75° and a IFOV of 100 μrad. This design provides a pixel scale of 350 m at a flyby distance of 3500 km. In front of the TMA, a rotating mirror allows to alternatively point the surface of the Trojan and the two calibration targets: (a) deep space and (b) a thermally regulated black body at about 150 K. A block diagram of THERMAP is presented in Fig. 12 identifying the different sub-systems.

THERMAP operates like a framing camera, taking thermal images while pointing the object. A pointing stability of 50 μrad (1/2 pixel) over a few

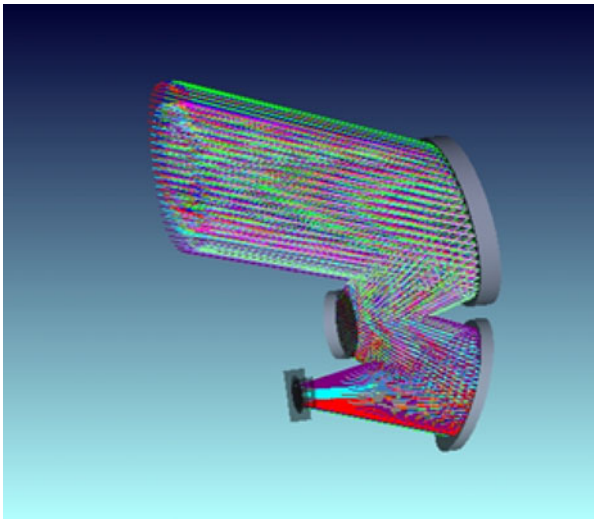

Fig. 11 Conceptual design of the TMA telescope of THERMAP

seconds is required. To guarantee a good accuracy of the temperature measurements (better than 1 K), a calibration cycle is performed regularly, using the rotating mirror, by alternatively pointing the two calibration targets. The exact duration and frequency of the calibration cycle will be investigated in the development phase, but it is typically short (less than 1 min) and repeated after each frame.

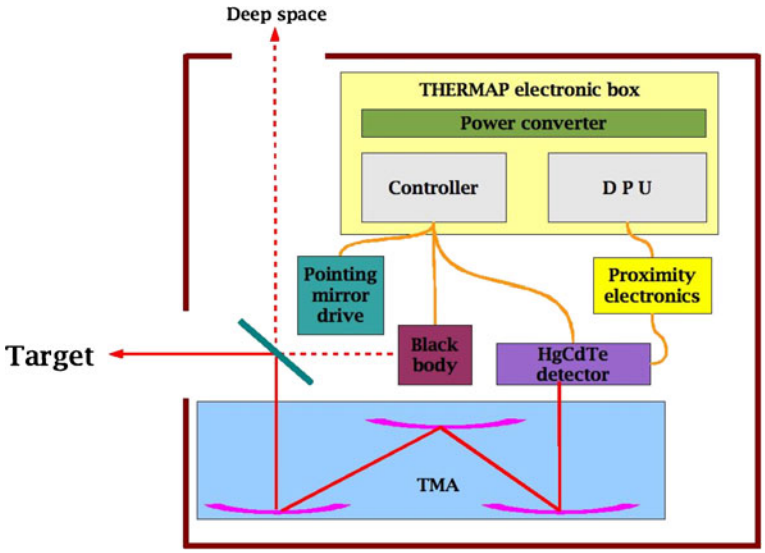

Fig. 12 THERMAP block diagram

The critical issues for the development of the THERMAP instrument are of thermal order, and in particular: (a) the passive cooling of the instrument to 110 K, (b) the active cooling of the detector from 110 K to 77 K, and (c) a good thermal stability during the operations.

4.1.4 The Trojan Thermal infrared Imaging Spectrometer (TROTIS)

TROTIS is a thermal infrared imaging spectrometer with an integrated radiometer. The scientific goal of TROTIS is to provide detailed information about the mineralogical composition of an asteroid's surface layer by measuring the spectral emittance in the spectral range 7–14 μm with a high spatial and spectral resolution. Furthermore TROTIS will obtain radiometric measurements in the spectral range from 7–40 μm to study the thermo-physical properties of the surface material.

The main science goals of TROTIS are:

- Map the composition with high spatial and spectral resolution
- Study the thermal properties of the asteroid
- Map the physical properties of the regolith

TROTIS builds on the heritage of the MERTIS instrument for the ESA Bepi-Colombo mission to Mercury. MERTIS is using an uncooled microbolometer array as detector for the spectrometer, to minimize the need for cooling in the hot environment around Mercury. TROTIS instead uses a cooled, 256 × 128 pixels HgCdTe detector to maximize the signal to noise ratio for the much colder surface of Trojan asteroids. While MERTIS has a FOV of 4° TROTIS has a FOV of 2° offering a higher spatial resolution.

The spectrometer of TROTIS is based on the Offner design with a micromachined grating. In combination with its detector TROTIS will cover the spectral range from 7–14 μm with a spectral resolution of 200 nm and a high spatial resolution. The radiometer is highly miniaturized and integrated in the slit plane of the spectrometer. The approach of combining a spectrometer and a radiometer with the same entrance optics provides synergies benefiting the scientific analysis. The fact that the surface temperature can be obtained independently from the spectral measurements allows removing ambiguities in the retrieval of emissivity values. The radiometer will further map thermal physical properties like thermal inertia, texture and grain size.

The instrument design is driven by a strong need for miniaturisation and a modular combination of the functional units at the same time. The units consist of the Sensor Head and the Electronics Unit with the pointing/calibration units in front of the optical entrance (Fig. 13). All sub-systems are designed (partially by cold redundancy) to withstand the extreme environmental conditions.

The sensor head structure contains the telescope, a Three Mirror Anastigmat with a 200 mm focal, f/ 2.5 (i.e., an aperture of 80 mm), and spectrometer optics, the bolometer and radiometer focal plates, its proximity electronics, the calibration devices (shutter and 170 K black body) and provides thermal interfaces to the Spacecraft to achieve required high thermal stability.

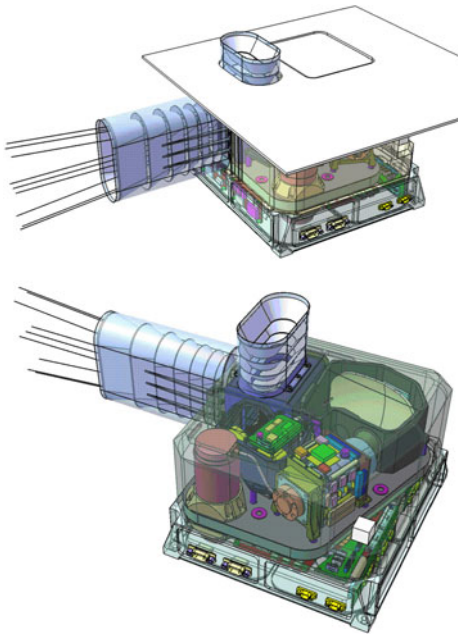

Fig. 13 Concept views of TROTIS, with radiator attached (*top view*) and without radiator to view the instrument interior (*bottom view*)

A pointing device is located at the optical entrance, which allows the incoming beam to come from four different sources, three for in-flight calibration purposes and the object view:

- deep space
- a blackbody at 170 K
- a spectral calibration target
- the asteroid surface

This segment as well as the Sensor Head is mounted into the Electronics Unit, which contains common cold redundant electronics for instrument control and power supply including electrical interfaces to the spacecraft, electronics for bolometer temperature stabilization, and the shutter electronics. It also serves as the housing for the sensor head and the pointing unit as well as the mounting interfaces for the two baffles.

The use of three calibration targets and an internal shutter provides a high accuracy and stability of the measurements. The 170 K black body and the deep space view are essential for the radiometric calibration, while the internal shutter allows removing contributions from the instrument itself as well as pixel to pixel variations on the detector. The spectral calibration target is a well-characterized sample that can be heated to different temperatures. This allows checking the spectral registration and verifying the performance of the instrument in-flight.

TROTIS will be typically operating in a mapping mode. In this mode the instrument will alternate between the three calibration views and the target

view. Spectral and radiometric data are obtained simultaneously. Binning in spectral as well as spatial directions can be performed in the instrument by software mode to optimize the signal to noise ratio based on the temperature of the target.

The instrument needs a view to cold space as calibration reference and a dedicated radiator for primary cooling of the detector. Further cooling will be achieved by a pulse tube cooler. Mounting interfaces as well as the position of the radiator can be adapted based on the spacecraft design. The instrument is equipped with a spacewire interface.

4.1.5 The radio science investigation

The RSI instrument is a coherent transponder designed to measure the Doppler shift of the X-band (8.4 GHz) carrier frequency of a 2-way radio-link between the spacecraft and the Earth with a precision of 0.02 mm/s at 60 s integration time. These Doppler shifts are used to reconstruct the fine velocity variations of the spacecraft induced by the gravitational attraction of the Trojan asteroid during the flyby event. This instrument is here foreseen to be used during an appropriate period around the flyby to ensure a coherent 2-way Doppler link between the spacecraft and Earth's based tracking stations with a stability characterized by an Allan deviation of 10^{-13} over 60 s.

The main scientific objectives of this instrument are:

- Determine the mass of the asteroid with an accuracy of a few percents
- Derive the bulk density of the asteroid by combining with a volume determination
- Constrain the interior structure of the asteroid (bulk porosity content)

The RSI instrument directly inherits from the LaRa instrument whose development was initiated in the frame of the ExoMars program [21]. A prototype has been delivered for the Preliminary Design Review (PDR) of the ExoMars mission, and the ESA review panel considered that the LaRa instrument has reached TRL 5.45.

The RSI transponder is housed in an aluminium box having dimensions of 154 × 130 × 45 mm (Fig. 14). It does not have a thermal control or a heater system, but it requires working in a thermal controlled environment for proper operations of its components (the operational temperature range extends from −50 C to 60 C). In its nominal mode, the total input power is 20 Watt. From these 20 W, 3 W are transferred into RF energy and 17 W are internally dissipated heat. The mass derived from the LaRa design is 0.75 kg.

The transponder electronics box provides connections to the spacecraft Data Handling Subsystem (CDH), the Electrical Power Subsystem (EPS), and the Thermal Control Subsystem (TCS), see Fig. 15. Only commands and housekeeping data are transferred, and CAN BUS is not used since no scientific data are transferred to the spacecraft platform.

The LaRa transponder was designed with a low gain antenna (Fig. 15), but using instead the high gain antenna (HGA) of the spacecraft is mandatory

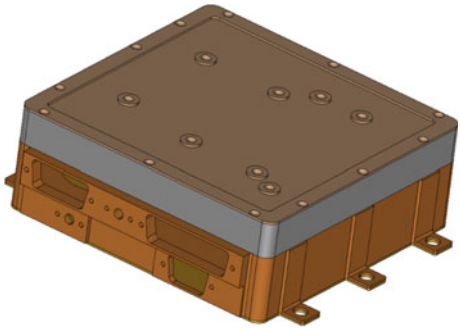

Fig. 14 The RSI transponder

in the present mission to ensure a sufficient link budget of the radio-link at Earth–Jupiter distance and therefore to provide Doppler measurements with a precision of 0.02 mm/s at 60 s integration time. This performance has been estimated assuming that the noise affecting the Doppler measurements correspond to the nominal case of low level of the error sources induced by the media through which the radio-wave propagates (troposphere, ionosphere and solar plasma).

The tracking stations (DSN or ESTRACK networks) constitute the ground-segment of the RSI instrument as they perform the Doppler measurements. The HGA of the spacecraft must therefore be pointed to the Earth during the operations.

The accuracy on the asteroid mass determination can reach 1%, depending upon the density and size of the targeted-asteroid, on the spacecraft–asteroid distance, and the relative velocity at closest approach. It also depends upon the precise knowledge of the spacecraft orbit and of the ephemeris of the targets. The determination of the spacecraft position can be improved before the flyby event through a dedicated tracking campaign (ESA has gathered the relevant experience from the past successful flybys of Phobos by Mars Express and Lutetia asteroid by Rosetta). The Trojan asteroid ephemeris will be improved

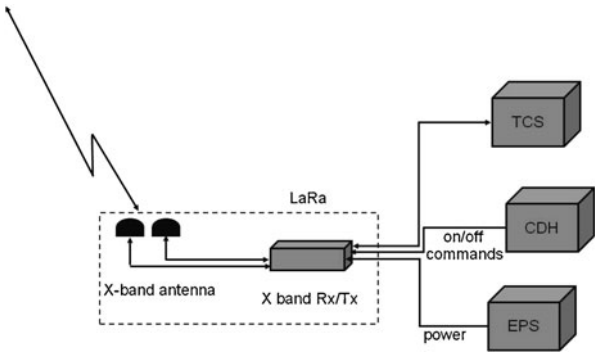

Fig. 15 Schematic diagram of the radio science investigation (derived from the LaRa experiment)

from the results of the GAIA mission and even refined using Earth-based dedicated astrometry campaigns in advance of the flyby events.

5 System requirements and spacecraft key issues

5.1 Architecture and Payload accommodation

The spacecraft is accommodated so as to allow a stable pointing of the instruments, a face for the mounting of the instruments, a large but compact solar array, and a large bi-propellant capacity. Figure 16 displays a typical spacecraft architecture for the Trojans' Odyssey mission based on the ExoMars Orbiter where the Descent Module top face would be replaced by the face on which the instruments are mounted. The top face is kept in shadow to provide for cold radiators. As studied on the Jupiter Ganymede Orbiter (JGO), this architecture has the capacity to accommodate the large solar arrays needed to produce the required power at up to 5.4 AU from the Sun. As the spacecraft has to be quite large to carry the large propellant tanks, the accommodation of the instruments and platform units is easy. This is a favorable factor for the control of schedule and costs.

The four remote sensing instruments require accommodation close to each other to meet the co-alignment specifications, unobstructed FOVs to the targets and open view to space for their radiators. They are therefore mounted altogether on the top face of the spacecraft (which is the face opposite to the launcher interface) with their optical axis parallel to this face. For the radio science investigation, the High Gain Antenna (HGA) shall be Earth-pointed during the flybys, thus requiring a two-axis pointing of the antenna while the spacecraft points towards the center of the asteroid (Fig. 17). The HGA is

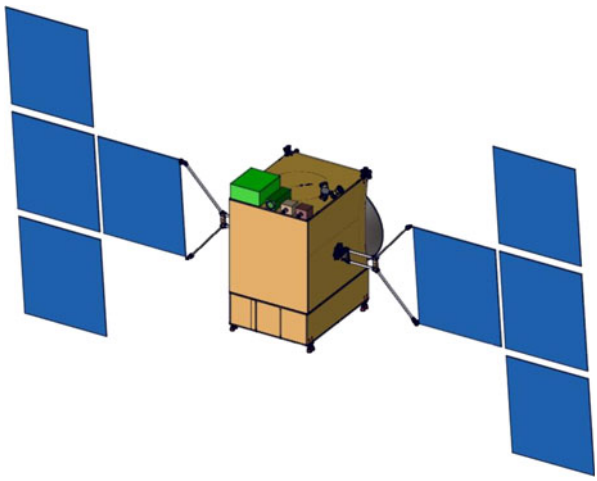

Fig. 16 A typical spacecraft architecture for the Trojans' Odyssey mission. The scientific instruments are mounted on the top face of the satellite (the *green box* being the Multicolor Camera and NIR spectrograph)

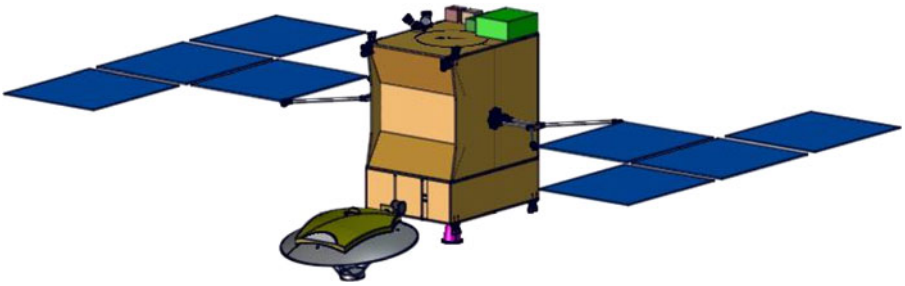

Fig. 17 Spacecraft typical configuration during a Trojan flyby. The HGA is pointed to the Earth to enable the radio science investigation during the flybys while the spacecraft points the instruments towards the object

implanted on the face opposite to the instruments common viewing direction as flybys will generally occur between the asteroid and Sun and Earth, so as to image its sunlit face.

The spacecraft cost must and can remain reasonable leading to:

- Prefer blowdown mode after Earth escape to simplify the propulsion;
- Use payload cameras for navigation to reduce platform cost;
- Limit Solar array surface as much as possible (30–40 m^2 typical);
- Limit communication subsystem complexity (recurring antennas, X-band) and communication power (35 W RF typical);
- Limit the number of instruments to be managed, and their mass (typically 5 instruments for a total mass of 50 kg).

5.2 Attitude and orbit control

The spacecraft is three-axis stabilized with fine pointing capacity for imaging, with required performances in line with current interplanetary missions. It is able to be slowly spun for cruise, safe modes and potential hibernation modes. The time spent quite close to the Sun for the fly-by of Venus will induce a thermal load to the spacecraft, leading to favor a Sun-pointing with HGA towards the sun like on Cassini or JGO.

These requirements can be globally achieved by using a classical suite of sensors and actuators, with star trackers, reaction wheels, and thrusters.

Propulsion needs are best met by MON/MMH bi-propellant, as this off-the-shelf technology will provide for the large Isp required by the mission. A 400-N engine will be used for Earth escape in the weeks following launch, with a 318 s Isp. Using this 400-N engine for the other maneuvers would be of benefit for the mass budget but would require many pressurization/insulation stages, adding to the complexity and cost. For this reason we baseline at this stage the definitive insulation of the 400-N engine after Earth escape and the use of

10-N thrusters in blowdown mode with an average Isp of 280 s for the orbital maneuvers. Indeed all these deep space maneuvers without significant gravity losses do not depend on the thrust level.

5.3 On-board data handling and telemetry

The on-board data handling will be a classical subsystem adequate to an interplanetary mission. As the mission consists in multiple flybys of planetary objects, a mass memory shall be implemented so as to download the science data after the flybys in order to limit operation costs and to avoid over sizing the communication subsystem. A classical 16 GB memory is deemed sufficient at that stage, to be further studied. The communication rate can be relatively slow as several weeks will statistically separate two consecutive flybys, allowing for an unconstrained downloading schedule. This leads to a classical interplanetary communication subsystem. The system is sized by the radio science needs. Cost considerations lead to recommend a large but off-the-shelf HGA of 2.2 m diameter in X-band recurring from Rosetta. Using the Ka-band would be beneficial both for the radio science investigation and data transmission but would add subsystem and operational costs, deemed not desirable at this stage.

5.4 Mission operations concept (ground segment)

A preliminary assessment of the mission operation concept is that Delta Differential One-way range (DDOR) measurements with 35 m diameter ground antennas (NASA Deep Space Network, or ESA Range network) are necessary for spacecraft orbit determination. A first estimate of DDOR performance led to an accuracy of 50 m on all axis in the worst case of a 6.2 AU spacecraft–target distance (Earth–Sun–Target conjunction although strictly speaking, DDOR measurements are not possible during such conjunctions). This accuracy is sufficient to meet the most demanding requirements of the Radio Science Investigation. However, should this later appears necessary, the determination of the spacecraft position can always be improved before the flyby by implementing a dedicated tracking campaign (ESA has acquired the relevant experience from the past successful flybys of Phobos by Mars Express and the Lutetia asteroid by Rosetta).

5.5 Estimated overall resources (mass and power)

The power is generated by a solar array sized by the platform need in between flybys. The solar array will benefit from on-going developments funded by ESA on Low Illumination Low Temperature (LILT) cells. Based on JGO study, a 32 m^2 array will provide an End-of-Life power of about 340 W (given the milder radiation environment) adequate to cover the needs of the

Table 4 Mass budget of the Trojans' Odyssey spacecraft

Items	Estimate in kg
Structure	175
Thermal control	45
Mechanisms	12
Communications	40
Data handling	19
AOCS	50
Propulsion	170
Power	190
Harness	55
Instruments	50
Total dry mass	806
Plus maturity margins	943
Plus system margin 20%	1132
Extra margin available beyond 20%	62
Allowable dry mass	1194
Helium mass for allowable dry mass	4
Total propellant for allowable dry mass	1872
Launch mass (excluding adaptor)	3070

platform (outside downlink) plus the stand-by consumption of the payload. A compact configuration with lateral panels is envisaged so as to guarantee the controllability of the spacecraft during the imaging phases. During the few hours that a flyby takes and which correspond to the peak consumption of the science payload, the spacecraft is not necessarily Sun-pointed and gets its power from batteries that are recharged within a few days following the flyby. In the same way, data downloads can, if needed, rely on both solar array and batteries. A 25 kg battery should cover the needs of both the operation of the payload during flyby and the subsequent data downlink phase, when the total consumption of the spacecraft increases up to about 550 W.

The assessment of the mass, benefiting from the references of the ExoMars and Jupiter Ganymede Orbiters, leads to the preliminary budget presented in Table 4. Adequate margins are already available at that stage with respect to the mission allocation. The quoted mass of propellant of 1872 kg assumes that the allowable dry mass will be saturated.

6 Technology development requirements

Because it relies on important heritage for both the spacecraft and the instruments, the proposed Trojans' Odyssey mission does not require any significant technology development and does not present any significant risks.

Regarding the payload, the proposed instruments are already at TRL$\geq$5, expect THERMAP currently at TRL 4. However, there is no doubt that THERMAP will be at TRL 5 by the end of the definition phase (phase A/B1). Indeed THERMAP is a simplified version of TROTIS, already at TRL$\geq$5.

All the elements on THERMAP have already been developed for TROTIS, and no new technology development is required to reach TRL 5. Finally, THERMAP and TROTIS will be developed in parallel, thus allowing a better synergy to reach higher TRL levels during the definition phase.

Regarding the mission and spacecraft technology, all subsystems are at TRL 7 or higher, except the LILT cells for Solar Array. Their development will be closely monitored so as to switch to the screened GaAs back-up solution in time if needed.

7 List of Co-investigators

Participants from ESA countries:
J. Agarwal (NL), A. Barucci (FR), M. Birlan (FR), R. Brunetto (FR), M. T. Capria (IT), B. Carry (ES), A. Cellino (IT), E. Cloutis (CA), F. Colas (FR), V. DaDeppo (IT), B. Davidsson (SE), V. Dehant (BE), J. De Leon (ES), A. Delsanti (FR), A. Doressoundiram (FR), R. Duffard (ES), A. Fitzsimmons (UK), S. Fornasier (FR), S. Green (UK), P. Gutierrez (ES), A. Harris (DE), D. Hestroffer (FR), S. Hviid (DE), L. Jorda (FR), M. Kaasalainen (FI), J. Knollenberg (DE), E. Kuehrt (DE), P. Lacerda (UK), Y. Langevin (FR), C.-I. Lagerkvist (SE), F. Leblanc (FR), C. Leyrat (FR), J. Licandro (ES), S. Lowry (UK), S. Marchi (IT), A. Maturilli (DE), F. Merlin (FR), P. Michel (FR), S. Mottola (DE), S. Mouret (DE), O. Mousis (FR), T. Mueller (DE), A. Nedelcu (RO), J. L. Ortiz (ES), N. Peixinho (PT), M. Popescu (RO), F. Poulet (FR), P. Pravec (CZ), E. Quirico (FR), P. Robutel (FR), P. Rochus (BE), A. Rossi (IT), B. Schmitt (FR), C. Snodgrass (DE), G. Strazzulla (IT), I. Toth (HU), J. Vaubaillon (FR), E. Vilenius (DE), D. Vokrouhlický (CZ), P. Wurz (CH)

Participants from the USA:
S. Besse (University of Maryland), R. Binzel (Massachusetts Institute of Technology), F.E. DeMeo (Massachusetts Institute of Technology), J. Emery (University of Tennessee), Y. Fernandez (University of Central Florida), R. Gaskell (Planetary Science Institute), W. Grundy (Lowell Observatory), A. Guilbert (UCLA), T. Hiroi (Brown University), D. Jewitt (UCLA), F. Marchis (SETI Institute), J-L. Margot (University of California), C. Olkin (Southwest Research Institute), M. Peck (Cornell University), G. Sarid (University of Hawaii), A. Stern (Southwest Research Institute), J. Sunshine (University of Maryland), H. Weaver (Johns Hopkins University Applied Physics Laboratory)

Participants from Japan:
N. Hirata (University of Aizu), S. Sasaki (National Astronomical Observatory of Japan), H. Yano (Japan Aerospace Exploration Agency), F. Yoshida (National Astronomical Observatory of Japan)

Participants from other countries:
C. Dumas (Chile), M. Gritsevich (Russia), M.D. Melita (Argentina)

8 Conclusions

Trojans are attracting growing attention from the planetary scientific community as it is realized that they hold the potential to unlock the answers to fundamental questions about planetary migration, the late heavy bombardment, the formation of the Jovian system, the origin and evolution of trans-neptunian objects, and the delivery of water and organics to the inner planets. Space missions are being studied in the USA and in Japan and mission proposals have either already been submitted or are under way. We emphasize that the "Planetary Sciences Decadal Survey" released by NASA on 7 March 2011 has listed among its priorities a "Trojans Tour" mission clearly illustrating the burning interest of the planetary community for these objects.

Our study demonstrates that the proposed Trojans' Odyssey reconnaissance, multiple flyby mission aimed at visiting several objects, typically five Trojans (and possibly one Hilda), is feasible in Europe with available resources. It does not require any significant technology development and does not present any significant risks. The only open issue regarding the existence of suitable orbital trajectories has further been recently solved by a study performed by CNES [15] that validates the proposed solution of multiple flybys. Based on the 3000 currently known asteroids in the L4 cloud, the simulation shows that there are 36 trajectories that achieve 4 flybys and 2 that achieve 5 flybys, all with flyby velocities in the range 5 to 6 km/sec. Considering that the forthcoming sky surveys (PanStarrs) will significantly increase the number of known objects, both the number of possible trajectories and visited targets will increase as well, thus easing the mission orbital constraints (e.g., launch date) and enhancing the science return.

Acknowledgements The proposal has benefited from contributions of the following persons: J. Fontdecaba-Baig and E. Benet of Thales Alenia Space (Cannes), D. Carbonne, P.-W. Bousquet, D. Fournier, M.-C. Desjean of CNES (Toulouse), J. Berthier of IMCCE (Paris), A. Mithra of AtoS (Toulouse), M. Le Roux, and J. Jaussel.

References

1. Gomes, R., et al.: Nature **435**, 466 (2005)
2. Morbidelli, A., et al.: Nature **435**, 462 (2005)
3. Tsiganis, K., et al.: Nature **435**, 459 (2005)
4. Lacerda, P., Jewitt, D.: AJ **133**, 1393–1408 (2007)
5. Drouart, A., et al.: Icarus **140**, 129–155 (1999)
6. Morbidelli, A., et al.: Planet. Sci. **35**, 1309–1320 (2000)
7. Dalton, J.B.: Space Sci. Rev. **153**, 219–247 (2010)
8. Takato, N., et al.: Science **306**, 2224–2227 (2004)
9. Filacchione, G., et al.: Icarus **206**, 507–523 (2010)

10. Emery, J.P., et al.: Icarus **182**, 496–512 (2006)
11. Vernazza, P., et al.: Icarus **207**, 800–809 (2010)
12. Strazzulla, G., et al.: Icarus **91**, 101–104 (1991)
13. Belton, M.J.S., Melosh, J.: Icarus **200**, 280–291 (2009)
14. Snodgrass, C., et al.: Nature **467**, 814–816 (2010)
15. Canalias, E., et al.: AAS/AIAA Astrodynamics Specialists Conference. AAS 11–481 (2011)
16. Dohlen, K., et al.: Optical Eng. **35**, 1150 (1996)
17. Jorda, L., et al.: Astron. Astrophys. **487**, 1171–1178 (2008)
18. Hampton, et al.: Space Sci. Rev. **117**, 43 (2005)
19. Cheng, A.F., et al.: Space Sci. Rev. **140**, 189 (2008)
20. Hiesinger, H., Helbert, J., MERTIS Co-I Team: Planet. Space Sci. **58**, 144–165 (2009)
21. Dehant, V., et al.: Planet. Space Sci. **57**, 1050–1067 (2009)